Prediction and Control of Ground Deformations for Mechanized Tunneling in Clays with Mixed Face Conditions

Andrew J. Whittle(✉) and Vasiliki Founta

Massachusetts Institute of Technology, Cambridge, USA
ajwhittl@mit.edu

Abstract. This paper describes a new methodology for predicting and controlling ground movements for a tunnel that traverses an interface between two clay layers of contrasting shear strength and stiffness. We use non-linear finite element analyses to investigate effects of face pressure on tunnel face stability and steady state ground surface deformations. This leads to a series of design charts linking soil properties (undrained shear strength and stiffness), stratigraphy (layer interface), tunnel cover depth and mechanized control parameters (face and grout pressure). The methodology has been validated for a recent case study where EPB tunnels traverse an interface between stiff clay (Old Alluvium) and soft, Marine clays. The proposed methodology successfully uses the measured face pressures to predict ground movements for these mixed face conditions. Further generalization of the method is now needed to represent mixed face conditions with contrasting permeability.

1 Introduction

Closed-face Earth Pressure Balance (EPB) tunnel boring machines have been very effective in reducing risks associated with urban tunneling projects. The EPB design controls face pressures within a sealed cutter-head chamber that is filled with the excavated soil. As the machine advances the soil is mixed with conditioning agents to produce a low shear strength paste (undrained shear strength, s_u = 20–30 kPa; Mair 2008) that can flow through the screw conveyor, Fig. 1a. Tunnel excavation inevitably generates sources of ground movements due to stress relief at the excavated face, overcutting and ploughing of the shield, complex boundary conditions around the tail void and deformations of the segmental lining system. The EPB operation aims to control ground deformations through the face pressure (and machine advance rate) and through grouting (and grout pressures) applied within the tail void. While the performance of EPB machines has been very impressive, especially in homogenous ground conditions (e.g., Ieronymaki et al. 2018), the control of ground movements is particularly difficult when the TBM encounters an interface between materials of contrasting shear strength, stiffness and permeability. These mixed face conditions can result in excessive settlements (including the creation sinkholes; Shirlaw 2008), due to over-excavation at the face, water inflow, abnormal or excessive equipment wear and time delays during construction (Zhao et al. 2007).

T. Triantafyllidis (Ed.): *Recent Developments of Soil Mechanics and Geotechnics in Theory and Practice*, LNACM 91, pp. 267–280, 2020.
https://doi.org/10.1007/978-3-030-28516-6_14

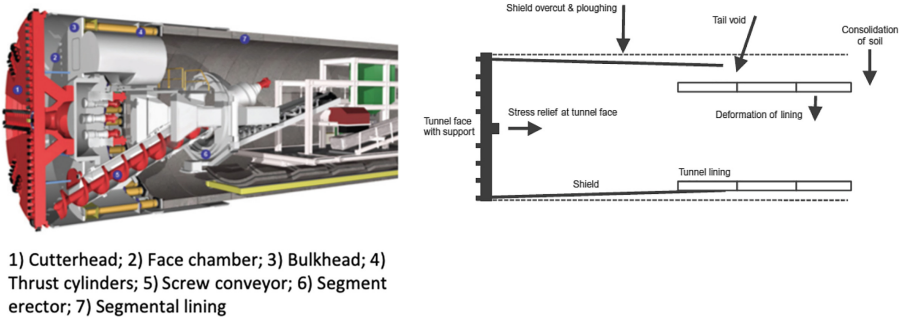

Fig. 1. Closed-face EPB shield tunneling (adapted from Möller 2006)

The goal of this study was to develop a simplified framework for predicting the ground movements as a function of face pressures for tunneling across an interface between clay layers of contrasting strength and stiffness. We have developed a semi-empirical method based on non-linear finite element analyses and illustrate its application from a recent tunneling project. The analysis framework provides a predictive framework that can be used to establish target face pressures during EPB operations.

2 Methodology

In prior studies we have investigated predictions of EPB tunnel-induced ground movements using a variety of soil models and representations of the ground-TBM interactions (Founta et al. 2013; Founta 2017). These studies have shown that relatively simple representations of the tunnel advancement process through incremental stepping of the boundary conditions (Möller 2006) achieve comparable predictions of ground movements to more complex representations of the TBM as a separate structural body. Similarly, the zone of soil plasticity occurs in the near-field of the TBM for well-executed mechanized tunneling such that relatively simple soil models can be used to estimate far field ground deformations (Ieronymaki et al. 2016). The current analyses use the linearly-elastic perfectly plastic (EPP) model to represent soil behavior and assume that ground movements caused by closed-face EPB tunnel construction can be estimated by considering 4 independent sources of settlement: (1) Face pressures; (2) Grout pressures within the tail void (the grout sets between the assembled segmental lining and the surrounding soil); (3) Overcutting due to the oversize cutterhead and tapered diameter of the shield that are used to reduce friction; and (4) Net buoyancy between the weight of the soil excavated within the tunnel cavity and the weight of the tunnel boring machine.

3 Face Stability

In order to use control settlements induced by tunneling, it is first necessary to establish the face pressure needed to ensure stability of the tunnel face. Sloan (2013) conducted 3D numerical limit analyses (NLA; upper and lower bounds) for the undrained stability of a lined-tunnel in a homogeneous clay with an unsupported heading of length, P. The results in Fig. 2a, show that the computed face pressures, σ_f/s_u, required for stability tend to underestimate the measured data from centrifuge model tests (Mair 1979), but the measured data are close to the computed Lower Bound results. Tschuchnigg et al. (2015) have subsequently done detailed comparisons that show very good agreement between numerical limit analyses (rigorous solutions for rigid plasticity) and stability analyses obtained by stress reduction methods (SRM) that are widely used in displacement-based finite element software. The SRM method, considers an initial equilibrium state and then progressively reduces the Mohr-Coulomb (c', ϕ') shear strength parameters. The SRM method resolves any stress points that violate the strength criterion (using standard stress point algorithms that redistribute the stresses) at any stage of the analysis until reaching a state where equilibrium can no longer be achieved. The factor of safety for the SRM is defined by:

$$FS = \frac{tan\phi'}{tan\phi'_{mob}} = \frac{c'}{c'_{mob}} = \frac{s_u}{s_{umob}} \tag{1}$$

where subscript *mob* refers to the mobilized shear strength parameters, and s_u is the undrained shear strength of the clay.

The current methodology uses the SRM (*phi-c* method; Brinkgreve and Bakker 1991) to compute face stability within the finite element program Plaxis 3D (Brinkgreve et al. 2012). These analyses are conducted through a simple two-step process that creates a tunnel heading within a large FE model of the ground: (i) Tunnel excavation is simulated by simultaneous de-activation of soil elements within the tunnel cavity and activation of the plate-elements for the tunnel lining. The tunnel face is equilibrated at a constant face pressure representing average total stresses at the springline (depth, H); (ii) stability is evaluated directly through strength reduction.

Figure 2a shows that the current SRM analyses match closely the Lower Bound (LB) results presented by Sloan (2013). The mechanisms of failure vary with tunnel cover depth (C/D) for the EPB tunnel boring machine (where P/D = 0). Figure 2b shows further comparisons of the face stability number computed by SRM with results from prior limit analyses. The results show that stability number converges to N = 13 for C/D $\geq$ 3.5 corresponding to a failure mechanism for a deep tunnel that does not extend up to the ground surface.

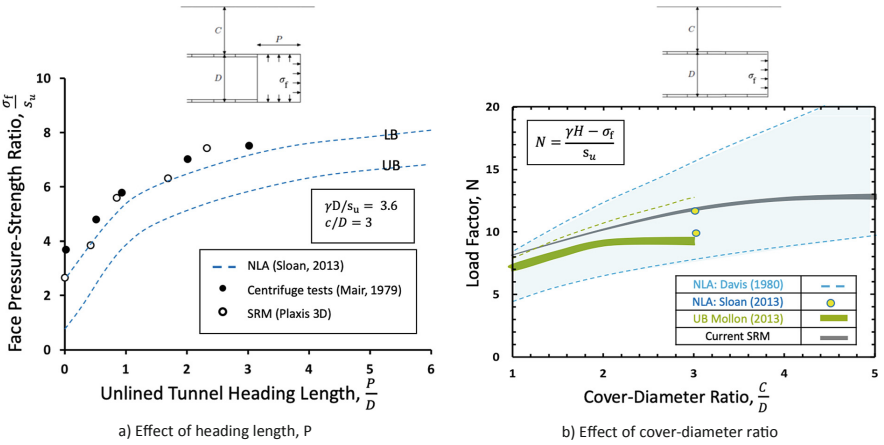

Fig. 2. Analysis of undrained face stability of lined tunnels in homogeneous clay

Strength reduction analyses can be readily extended to consider the face stability for mixed face conditions. For example, Fig. 3 illustrates the computed failure mechanisms for a tunnel heading that encounters two clay units of contrasting undrained shear strength. Here we consider a system comprising a soft clay (layer T) overlying a stronger clay (layer B) with undrained strength ratio, $s_{uB}/s_{uT} \geq 1$. The interface between the two layers bisects the tunnel face and is characterized by the embedment ratio, $-1 \leq D_T/D \leq 1$. The strength reduction method assumes the same factor of safety in both clay units. Figure 3 illustrates the face pressure required for stability for a shallow tunnel (C/D = 1) at a prescribed undrained strength ratio $s_{uB}/s_{uT} = 5$. The results are presented as functions of the embedment ratio, D_T/D, and strength of the upper clay unit, $s_{uT}/\gamma H$ (where H is the depth to the springline). For a given embedment depth, face pressure is only required when the strength of the upper clay unit is below a threshold value which increases with D_T/D. When the tunnel is fully embedded in the upper layer ($D_T/D = 1$) the face is stable for $\sigma_f/\gamma H = 0$ and $s_{uT}/\gamma H > 0.12$. In contrast, when the face is fully embedded in the lower clay ($D_T/D = 0.0$) the threshold strength of the upper unit is $s_{uT}/\gamma H = 0.04$, if the face pressure is increased to $\sigma_f/\gamma H = 0.5$ then the face is stable for $s_{uT}/\gamma H > 0.02$.

These results reflect differences in the face instability mechanisms associated with the two-layer system. Figure 4 illustrates the effects of the relative strength ratio, s_{uB}/s_{uT}, for a heading with C/D = 2 and $D_T/D = 0.25$. It is very interesting to observe the transition from a failure mechanism that extends across the full face of the tunnel and up to the ground surface (homogeneous case, $s_{uB}/s_{uT} = 1$), to a failure mechanism where the larger incremental deformations ($|\Delta u|/|\Delta u_{max}| > 0.75$) occur only within the upper soft layer ($s_{uB}/s_{uT} = 2$), or the majority of the mechanism ($|\Delta u|/|\Delta u_{max}| > 0.05$) is enclosed within the upper layer ($s_{uB}/s_{uT} = 10$).

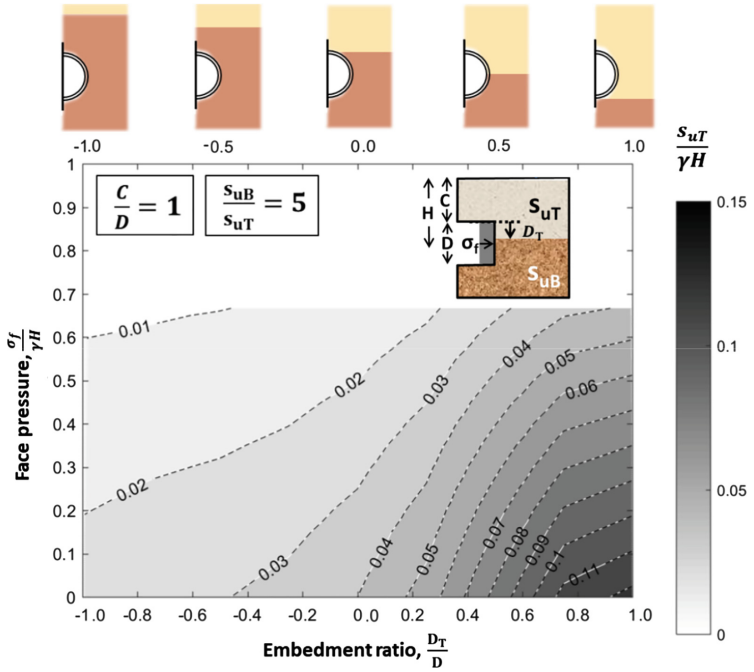

Fig. 3. Critical face pressure required to achieve stability for tunnel heading intersecting clay layers of contrasting strength computed by SRM

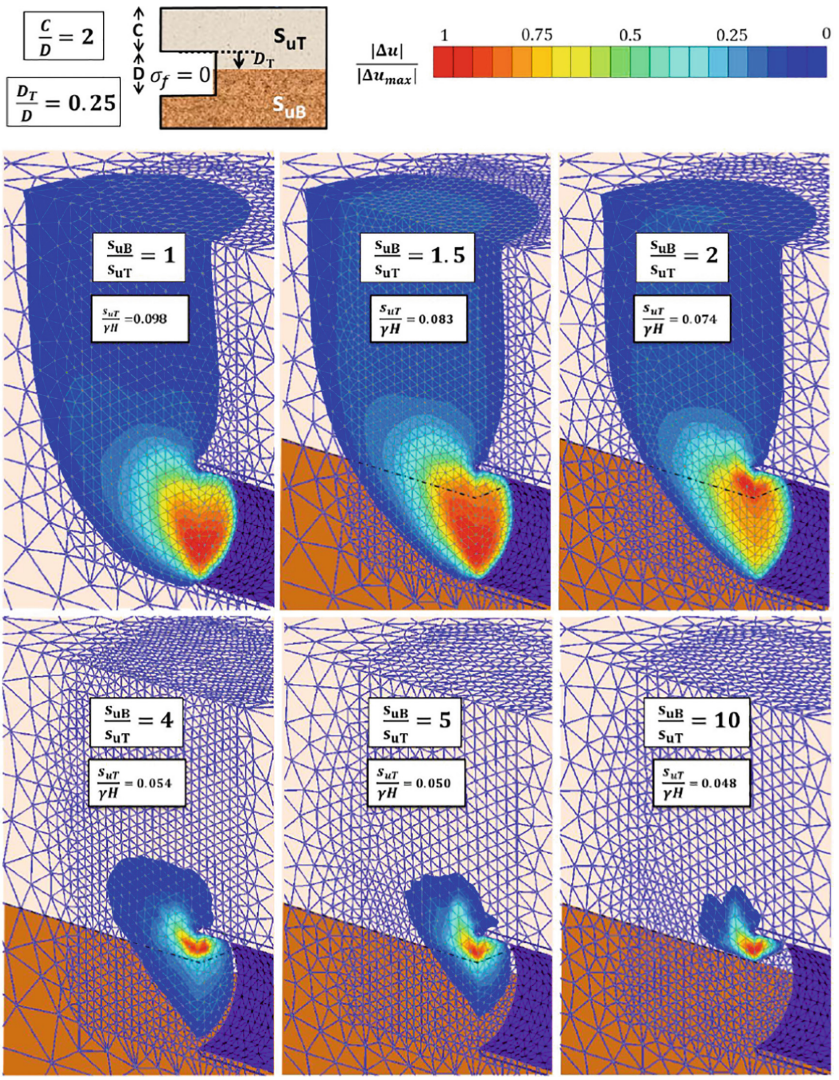

Fig. 4. Effect of relative strength ratio on collapse mechanisms for mixed face tunnel in clay

4 Ground Deformations Due to Face Pressures

The calculation of ground movements due to face pressures is accomplished using the same FE model used for face stability. The undrained shear behavior of the soil mass is represented by the EPP soil model (characterized by two parameters, G, s_u). We compute the net ground deformations associated with steady state advance of the TBM at a fixed face pressure. In practice, this is achieved by switching the frame of reference and integrating spatially the incremental movements associated with a single round of

advance for the tunnel heading. The initial state involves equilibration of the lined tunnel (with fixed radius) with the heading located in the mid-section of the FE ground model (the analyses consider a reference tunnel with 7 m diameter and a ground model with length 270 m). Far-field boundaries are located such that there are effectively zero incremental movements at each step of the advancing tunnel heading. Net deformations (surface settlements, u_z) are then computed by integrating the incremental movements (δu_z) over the length of the FE model for each step. Figure 5 shows that this process typically converges within 4–5 rounds of tunnel advance and hence, enables very efficient calculation of the net settlement. The effects of the shield conicity and tail void grouting are not considered in this analysis but are analyzed separately.

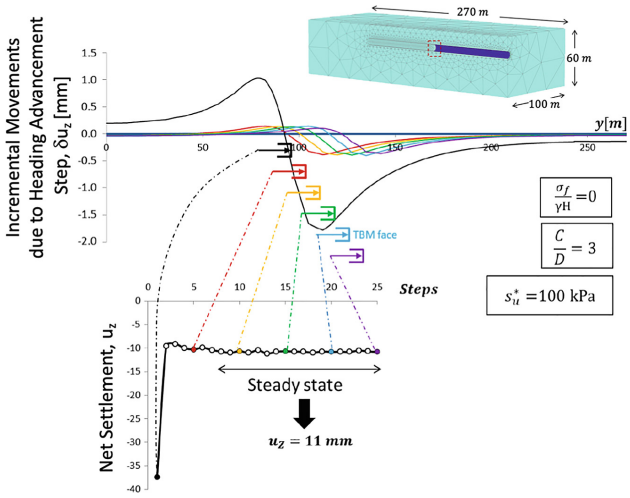

Fig. 5. Calculation of net settlement from incremental advances of heading at specified face pressure

Figures 6a and b illustrate typical predictions of the computed normalized net settlements for tunnels in homogeneous clays as functions of the face pressure and undrained shear strength at two cover ratios, C/D. The computed settlements are unbounded settlements for undrained strengths approaching critical values (s_u^c) obtained from the prior face stability calculations and converge to a range of residual deformations at high values of $s_u/\gamma H$. This behavior is well characterized by a rectangular hyperbola:

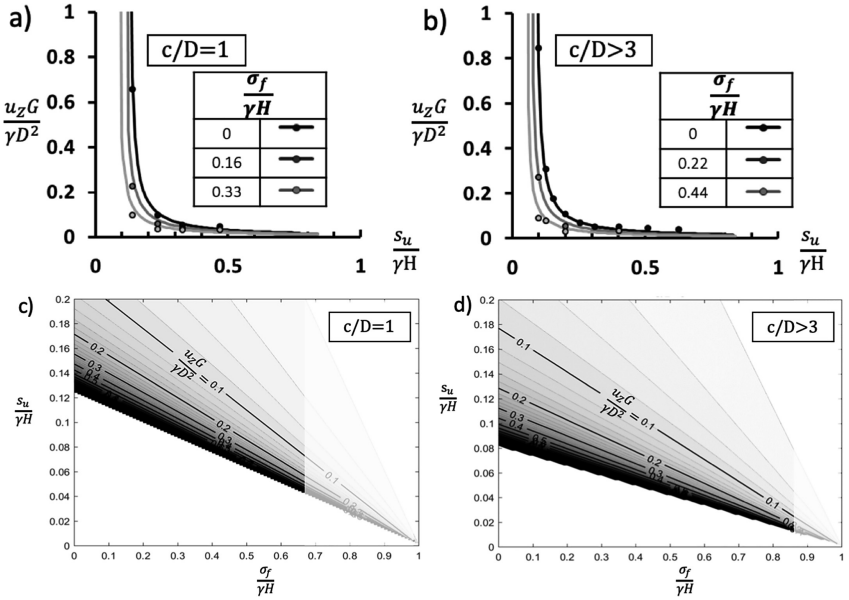

Fig. 6. Net settlements for tunnels in homogeneous clay (a), (b) computed results and curve fitting of data; (c), (d) derived design charts for estimating net settlement from undrained shear strength and face pressure

$$\frac{u_Z G}{\gamma D^2} = a\left(1 - \frac{\sigma_f}{\gamma \mathrm{H}}\right) / \left(\frac{s_u}{\gamma \mathrm{H}} - \frac{s_u^c}{\gamma \mathrm{H}}\right) \tag{2}$$

where the constant $a = a_{hom} = 0.012$, controls the residual net deformations and is obtained by least square fitting of the computed results.

Based on the known face stability results, Eq. 2 can be used to generate design charts that enable predictions of net settlements for specified combinations of (s_u and σ_f) as shown in Figs. 6c and d.

The same computational procedure can be used for 2-layer mixed face conditions with a constant interface embedment ratio, D_T/D. Figure 7 shows the computed net settlements as functions of the embedment ratio for a tunnel with C/D = 3 and undrained strength ratio, $s_{uT}/s_{uB} = 2$. These results highlight the relationship between the undrained shear strength and the critical face pressure (where uncontrolled settlements). The remaining contours can be used to guide the selection of face pressure and hence, control the predicted surface settlements, u_z.

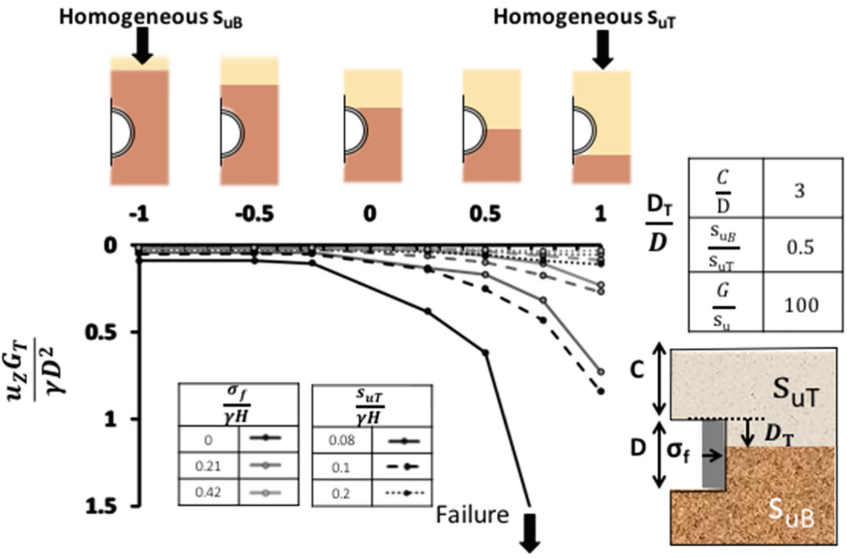

Fig. 7. Effect of tunnel embedment on computed settlements for two-clay layer mixed face conditions

A similar procedure can be used to relate face stability and surface settlements for mixed face conditions. Figure 7 summarizes the effects of the embedment ratio, D_T/D, on the computed surface settlements for a two clay layer system with $s_{uB}/s_{uT} = 2$ and $C/D = 3$ and selected values of the face pressure and undrained shear strength of the overlying clay ($\sigma_f/\gamma H$, $s_{uT}/\gamma H$). The surface settlements increase with the embedment ratio and failure occurs for the case (0.0, 0.08) at an embedment ratio, $D_T/D \approx 0.7$.

For given face pressure, the surface settlements can again be related to the undrained shear strength of the overlying clay (s_{uT} and the critical face pressure, $s_u^c/\gamma H$ as previously reported in Fig. 3) through a rectangular hyperbola function Eq. 2, where the constant is now a function of the embedment and undrained shear strength ratios, a (D_T/D, s_{uT}/s_{uB}).

Figure 8 shows the best fit values of the parameter a for the two-layer case (using the least squares method). The overall response is well-characterized by a logistic dose response curve (e.g., Joseph and Yang 2010) with input parameters as follows:

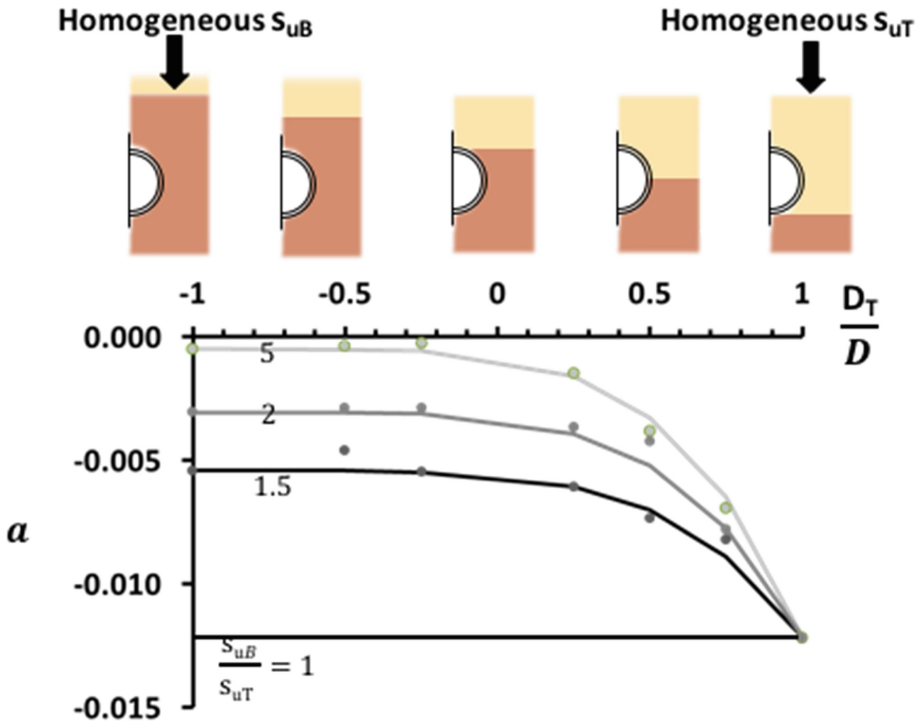

Fig. 8. Empirical interpretation of constant a in Eq. 2 for tunnels with mixed face conditions. Computed results in symbols, fitted logistic dose response function in solid lines

$$a = a_{hom}\left\{\left(1-\left(\frac{s_{uT}}{s_{uB}}\right)^2\right)\left[\left(\frac{\frac{D_T}{D}+1}{2}\right)^5-1\right]+1\right\} \tag{3}$$

Based on these results it is now possible to predict the surface settlements as a function of the embedment ratio, reference undrained strength ($s_{uT}/\gamma H$) and face pressure ($\sigma_f/\gamma H$). Figure 9 illustrates the resulting design charts. These results show how the face pressure must be increased in order to control surface settlements as the tunnel transits through the mixed face condition between the two clay layers.

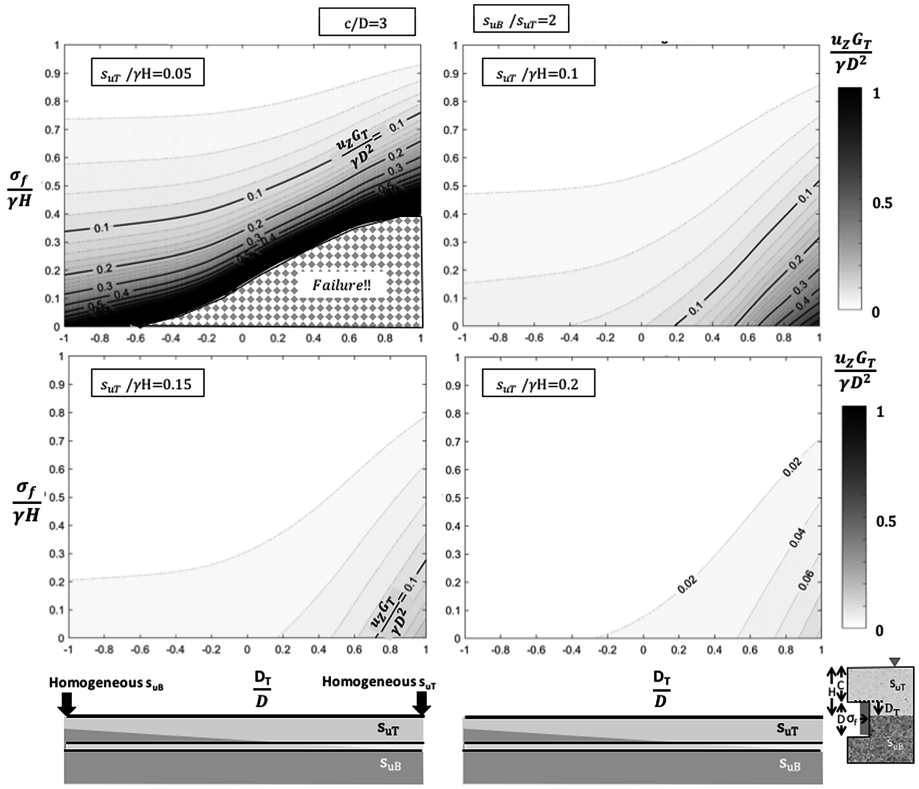

Fig. 9. Proposed design charts for predicting the effects of face pressure on the control of surface settlements of a tunnel heading for a two-layer, mixed face clay condition

5 Analyses of Other Sources of Ground Deformations

As indicated in the introductory section we have considered three other potential sources of ground deformations associated with EPB tunneling: The effects of grouting within the tail void are simulated by an independent analytical model following a methodology very similar to that used for face pressures. We first consider stability conditions for the tail void i.e., the critical undrained shear strength for an unsupported annulus (zero grout pressure over one-round length of segmental lining behind the shield) and then compute surface settlements as a function of the grout pressure that is actually applied within this void. The relationship between the surface settlement and grout pressure is similarly represented by a rectangular hyperbolic function that is calibrated to the computed results for each ground condition.

Effects of overcutting and buoyancy can be estimated from the known cavity contraction associated geometry of the TBM shield and cutterhead and from the ratio of the TBM to excavated soil weight, respectively. Far field ground deformations due to these effects can be well-estimated from elastic theory using analytical solutions (Pinto and Whittle 2014).

6 Model Evaluation

The goal of the proposed methodology is to provide a reliable tool that can enable reliable control of ground deformations for mechanized tunneling through mixed face conditions through adjustment of face and grout pressures. In order to assess the predictive accuracy of the proposed method we have applied the methodology directly to a number of archived case studies.

Su (2015) presents extensive data on ground settlements and tunnel face pressures for twin 6.6 m diameter EPB tunnels in Singapore (DTL Contract C933), Figs. 10a, b, and c. The section of interest concerns 900 m of the alignment where the twin tunnels were constructed sequentially one above the other (TBM 1 with C/D $\approx$ 5.0 $\pm$ 03; TBM 2, C/D = 3), such that ground movements can be considered separately for each bore. The tunnels transition from full embedment within the underlying Old Alluvium (stiff clay) layer with s_u = 250 kPa and G/s_u = 200; into a much weaker Marine clay with $s_u \approx 40$ kPa (i.e., $s_{uB}/s_{uT} = 6.25$), Fig. 10c. Figure 10b shows that the contractors increased the face pressure as each TBM advanced towards the marine clay. This is particularly notable for TBM2 where face pressure was increased from σ_f = 2.5 bar–4.5 bar, but this was not sufficient to control the observed ground settlements (measured directly above the tunnel crown) that increase from u_z = 3–5 mm in the Old Alluvium up to 20–25 mm in the Marine clay, Fig. 10a (Sharma 1999).

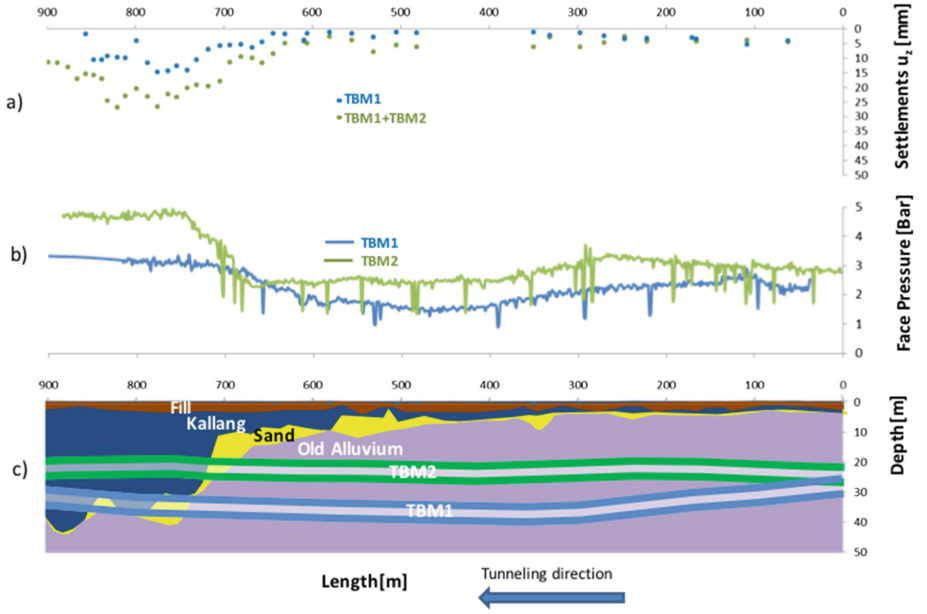

Fig. 10. Surface settlements, face pressures and stratigraphy for EPB tunnel construction at DTL C933 (after Su 2015)

The deformations at each location were predicted by superimposing the calculated displacements due to the TBM contraction and those due to the applied face pressure, Fig. 11. For the purpose of this comparison, we decided to ignore the effect of the grout pressure as high grout pressures were applied over this segment (close or equal to the geostatic stresses), resulting in minimal disruption of the surface.

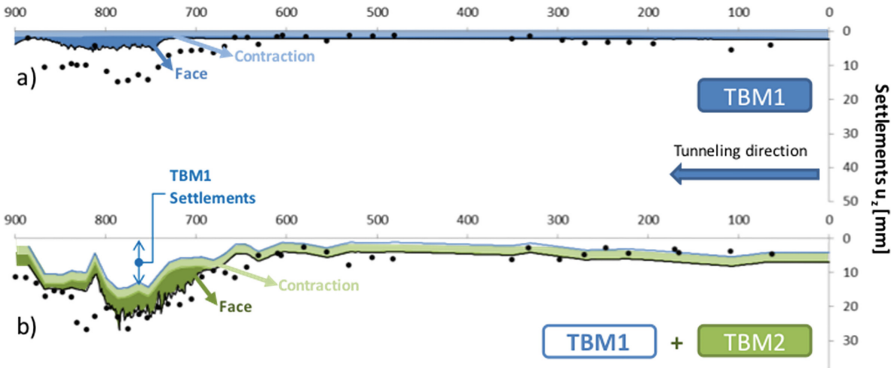

Fig. 11. Comparison of predicted and measured surface settlements due to EPB tunnel construction, DTL C933

Overall, there is a good agreement between the predictions and the measured surface settlements, Figs. 10a and b. For TBM1, there is excellent agreement for the segments where the EPB is embedded within the stiff old alluvium formation (0 to 700 m). However, the analysis underestimates settlements as the heading progresses into the Marine clay (Fig. 11a). This result may by caused by the presence of pockets of sand (unit F1). The performance of the shallower bore, TBM2, is much more reliably estimated (Fig. 11b; only one pocket of sand at around 700 m) showing the potential of the proposed analyses to represent realistically the ground movements.

7 Conclusions

This paper has demonstrated the use of computational models based on 3D finite element analyses to predict the relationship between tunnel geometry (C/D, DT/D), control parameters (face pressure, $\sigma_f/\gamma H$ and grout pressure), soil properties ($s_u/\gamma H$, s_{uB}/s_{uT}) and surface settlements ($u_z G/\gamma D^2$) for EPB tunnels. The current analyses have focused on a two-layer clay system, but the methodology employed in this work is general and can be applied to more complex ground profiles. The key assumption is that control of face pressures ensures that tunnel construction induces relatively small deformations in the surrounding ground (while face stability conditions are accurately estimated by SRM). The proposed methodology offers a tool that can be used to assess the control of ground movements based on a series of relatively simple numerical analyses. Initial evaluations for a recent case study in Singapore show that the proposed framework can provide credible predictions of performance and hence, could be used to design the face pressures for mixed face conditions.

Acknowledgements. This research was supported in part by Ferrovial-Agroman through the MIT-Ferrovial research Program and by the MIT-Singapore Alliance for Research and Technology (SMART) through the Center for Environmental Sensing and Modeling. The second Author is also grateful for support for the Onassis Foundation. We would also like to thank Dr Thiri Su (LTA) for her assistance in interpreting data from the DTL C933 project.

References

Brinkgreve, R.B.J., Engin, E., Swolfs, W., Waterman, D., Chesaru, A., Bonnier, P., Galavi, V.: Plaxis 3D 2012, Users Manual. Plaxis, Delft (2012)

Brinkgreve, R.B.J., Bakker, H.L.: Non-linear finite element analysis of safety factors. In: Proceedings of the International Conference on Computer Methods and Advances in Geomechanics, pp. 1117–1122. Balkema (1991)

Founta, V., Ninic, J., Whittle, A.J., Meschke, G., Stascheit, J.: Numerical simulation of ground movements due to EPB tunnelling in clay. In: Proceedings of the 3rd EURO:TUN Conference: Computational Methods in Tunneling and Subsurface Engineering, Bochum, Germany (2013, in print)

Founta, V.: Prediction of instability and ground movements during tunnel construction in non-homogeneous conditions. Ph.D thesis. Massachusetts Institute of Technology, Cambridge, MA (2017)

Ieronymaki, E.S., Whittle, A.J., Simic, D.: Interpretation of greenfield ground movements caused by mechanized tunnel construction. ASCE J. Geotech. Geoenviron. Eng. (2016). https://doi.org/10.1061/(ASCE)GT.1943-5606.0001632

Ieronymaki, E., Whittle, A.J., Einstein, H.H.: Comparative study of the effects of three tunneling methods on ground movements in stiff clay. Tunn. Undergr. Space Technol. **74**, 167–177 (2018)

Joseph, D.D., Yang, B.H.: Friction factor correlations for laminar, transition and turbulent flow in smooth pipes. Physica D **239**(14), 1318–1328 (2010)

Mair, R.J.: Centrifuge modeling of tunnel construction in soft clay. Ph.D thesis. Cambridge University (1979)

Mair, R.J.: Tunnelling and geotechnics: new horizons. Géotechnique **58**(9), 695–736 (2008)

Möller, S.C.: Tunnel induced settlements and structural forces in linings. Ph.D thesis. Institute of Geotechnical Engineering, University of Stuttgart (2006)

Pinto, F., Whittle, A.J.: Ground movements due to shallow tunnels in soft ground: 1. Analytical solutions. ASCE J. Geotech. Geoenviron. Eng. **140**(4), 0401.3040 (2014)

Sharma, J.S., Chu, J., Zhao, J.: Geological and geotechnical features of Singapore: an overview. Tunn. Undergr. Space Technol. **14**(4), 419–431 (1999)

Shirlaw, J.N.: Mixed face conditions and the risk of loss of face in Singapore. In: International Conference on Deep Excavations (ICDE 2008), Singapore, p. 7 (2008)

Sloan, S.W.: Geotechnical stability analysis. Géotechnique **63**(7), 531–572 (2013)

Su, T.: Study on ground behavior associated with tunneling In mixed-face soil condition. Ph.D thesis. National University of Singapore, Singapore (2015)

Tschuchnigg, F., Schweiger, H.F., Sloan, S.W., Lyamin, A.V., Raissakis, I.: Comparison of finite-element limit analysis and strength reduction techniques. Géotechnique **65**(4), 249–257 (2015)

Zhao, J., Gong, Q.M., Eisensten, Z.: Tunnelling through a frequently changing and mixed ground: A case history in Singapore. Tunn. Undergr. Space Technol. **22**(4), 388–400 (2007)